Impacts of New Suggested Ferroresonance Limiter on the Stability Domain of Ferroresonance Modes in Power Transformers Considering Metal Oxide Surge Arrester Effect

H. Radmanesh* and M. Rostami**

Abstract: This paper studies effect of new suggested ferroresonance limiter on controlling ferroresonance oscillation in the power transformer including metal oxide surge arrester (MOSA). A simple case of ferroresonance circuit in a three phase transformer is used to show this phenomenon and three-phase transformer core structures including nonlinear core losses are discussed. The effect of MOSA and ferroresonance limiter on the onset of chaotic ferroresonance and controlling chaotic transient in a power transformer including nonlinear core losses has been studied. It is expected that these ferroresonance Limiter generally cause into ferroresonance control. Simulation is done on a power transformer rated 50 MVA, 635.1 kV with one open phase. The magnetization characteristic of the transformer is modelled by a single-value two-term polynomial with q=7, 11. The core losses are modelled by third order in terms of voltage. The simulation results reveal that connecting the MOSA and ferroresonance limiter to the transformer, exhibits a great impact on ferroresonance overvoltages. Significant effect on occurring chaotic ferroresonance, the range of parameter values that may lead to overvoltage and magnitude of ferroresonance overvoltage is obtained and showed.

Keywords: Metal Oxide Surge Arrester, New Suggested Ferroresonance Limiter, Control of Chaos, Bifurcation, Ferroresonance, Power Transformers, Nonlinear core losses effect.

1 Introduction

The ferroresonance is typically initiated by saturable magnetizing inductance of a transformer and a capacitive distribution cable or transmission line connected to the transformer. In most practical situations, ferroresonance results in dominated currents, but in some operating "mode", may cause significant high values distorted winding voltage waveform, which is typically referred to as ferroresonance. Although occurrences of the "resonance" occurring does involves a capacitance and an inductance, but there is no definite resonant frequency ferroresonance occurrence for it. In this phenomenon, more than one response is possible

for the same set of parameters, and drifts or transients may cause the response to jump from one steady-state response to another one. Its occurrence is more likely to happen in the absence of adequate damping. Research on ferroresonance in transformers has been conducted over the last 80 years. The word ferroresonance first appeared in the literature in 1920 [1], although papers on resonance in transformers appeared as early as 1907 [2]. Practical interests had been shown was in the 1930s, when it is shown that the use of series capacitors for voltage regulation could cause ferroresonance in distribution systems [3]. Ferroresonant behavior of a 275 kV potential transformer, fed from a sinusoidal supply via circuit breaker grading capacitance, is studied in [4]. The potential transformer ferroresonance from an energy transfer point of view has been presented in [5]. A systematical method for suppressing ferroresonance at neutral-grounded substations has been studied in [6]. A sensitivity study on power transformer ferroresonance of a 400 kV double circuit has been reviewed in [7]. A novel analytical solution to the fundamental ferroresonance has been given in [8]. In that paper, the problem with the traditional excitation characteristic (TEC) of nonlinear inductors has been

investigated. The TEC contains harmonic voltages and/or currents. The Stability domain calculations of the period-1 ferroresonance have been investigated in [9]. The application of the wavelet transform and MLP neural network for the ferroresonance identification is used in [10]. The impact of the transformer core hysteresis on the stability domain of ferroresonance modes is studied in [11]. A 2-D finite-element electromagnetic analysis of an autotransformer experiencing ferroresonance is given in [12]. A new modeling of transformers enabling to simulate slow transients more accurate than the existing models in Simulink/MATLAB is presented in [13]. Controlling ferroresonance oscillations in potential transformer considering nonlinear core losses and the circuit breaker shunt resistance effect has been investigated in [14] and [15]. The effect of linear and nonlinear core losses on the onset of chaotic ferroresonance and duration of transient chaos in an autotransformer has been studied in [16]. Fault type estimation in power systems has been investigated in [17]. This paper presents a novel approach for fault type estimation in power systems. The fault type estimation is the first step to estimate instantaneous voltage, voltage sag magnitude and duration in a three-phase system at fault duration. Stochastic congestion management considering power system uncertainties is done in [18]. In this paper, a stochastic programming framework is proposed for congestion management considering the power system uncertainties. Mathematical proof for the minimized stray fields in transformers using auxiliary windings based on state equations for evaluation of fem results is studied in [19]. Reliability model of power transformer with ONAN cooling has been done in [20]. In this paper the reliability model of the power transformer with ONAN cooling is obtained. A new ZVZCS isolated dual series resonant dc-dc converter with EMC considerations is investigated in [21]. A novel ZVZCS isolated dual series-resonant active-clamp dc–dc converter is proposed to obtain high efficiency. The proposed converter employs an active-clamp technique, while a series-resonant scheme controls the output voltage with the complementary pulse width modulation controller. Investigation and control of unstable chaotic behavior using of chaos theory in electrical power systems has been studied in [22]. This paper consists of two sections: control and stabilizing method for chaotic behavior of converter is introduced in first section of this paper for the removal of harmonics caused by the chaotic behavior in current converter. In current paper, new suggested ferroresonance limiter is used an as compact circuit including one resistor, power electronic switch and control circuit for limiting and stabilizing of unstable and high amplitude ferroresonance oscillation. This resistance is connected to the grounding point of the power transformer and during ferroresonance occurrence; power electronic switch is connect the resistor to the transformer via controlling circuit. In this

work, MATLAB program is used to simulate ferroresonance and related phase plane and bifurcation diagrams. The result of the case study confirms that system states, lead to chaos and bifurcation occurs in proposed model. At first, MOSA is connected in parallel to the transformer in order to control ferroresonance. Then, the presence of the ferroresonance limiter tends to clamp the ferroresonance overvoltage, successfully. The ferroresonance limiter completely reduces the chaotic region for higher exponents. Simulation of system consists of two cases, at first, system modeling of power transformer including MOSA without connecting ferroresonance limiter and second, power system contains ferroresonance limiter. Finally compare the result of these two cases.

2 Power System Modeling Connecting MOSA

The power system studied here consists of a source feeding an unloaded power transformer with one supply conductors being interrupted as shown in Fig. 1 [23]. The transformer is then energized through the capacitive coupling with the other phases. Fig. 2 shows the circuits that feed the disconnected coil trough the capacitive coupling [23].

In order to derive the mathematical analysis of the above circuit, Thevenin's theorem is used to obtain an equivalent circuit. The equivalent capacitance can be found by decreasing the two remaining voltage source of phase 1 and 2. So, both corresponding ground
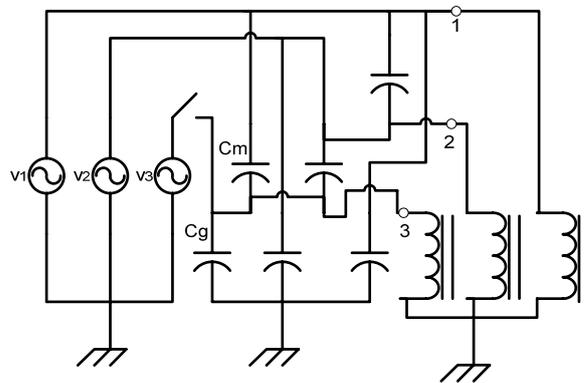
Fig. 1 Model of ferroresonance circuit including line capacitance.
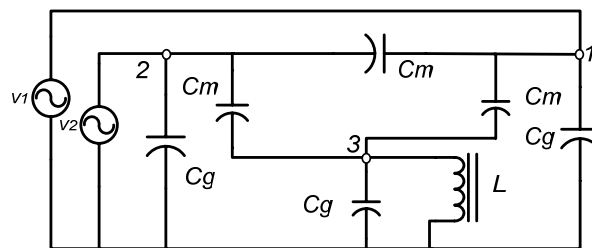
Fig. 2 Circuit that feeds disconnected coil.

capacitance and transformer windings are shorted and can be omitted as well. Therefore, the remaining equivalent circuit will consist of two mutual and one ground potential [23]. Under loaded operating conditions, the flux induced in the primary transformer windings are immediately compensated by the current flow in the secondary windings so that the core losses in the transformer can be omitted. However, in the case of an unloaded or very lightly loaded power transformer, current can develop in the secondary side and this causes the flux to emanate from the transformer leg and flow through the iron core. This in turn increases the transformer core losses and therefore it can no longer be neglected. Fig. 3 shows the final reduced equivalent circuit considering R as a core losses model [23].

Figure 3 shows the equivalent circuit of system which was described above. The magnetization branch is modeled by a nonlinear inductance in parallel with a nonlinear MOSA accordingly and represents the nonlinear saturation characteristic "φ-i_{Lm}" and nonlinear hysteretic and eddy current characteristics "v_m-i_{Rm}", respectively. The iron core saturation characteristic due to the explanation above is given by:

$$i_{Lm} = a\varphi + b\varphi^q \tag{1}$$

where, exponent q depends on the degree of saturation. It was found that for proper representation of the saturation characteristics of a power transformer, the exponent q may takes values 7 and 11. Fig. 4 shows graphical representation of these iron core characteristic for q =7, 11 [14].
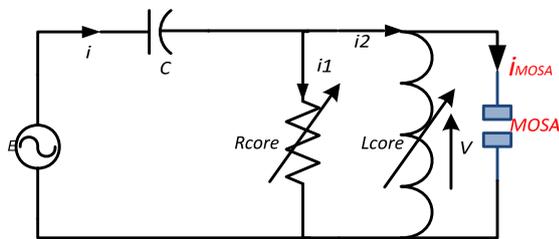
Fig. 3 Equivalent circuit of the power system including MOSA.
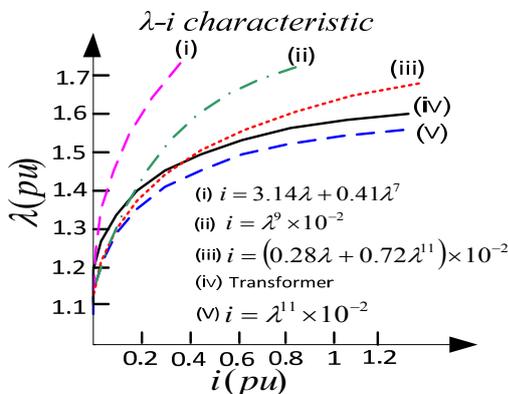
Fig. 4 Nonlinear characteristics of transformer core with different values of q [14].

3 Metal Oxide Surge Arrester Model

Surge Arrester is highly nonlinear resistor used to protect power equipment against overvoltages. MOSA can be arranged by cascading several metal oxide discs inside the same porcelain housing due to required protecting voltage. Size of each disc is related to its power dissipation capacity. The nonlinear V-I characteristic of each column of the surge arrester is modeled by combination of the exponential functions of the form

$$\frac{V}{V_{ref}} = K_i \left(\frac{I}{I_{ref}} \right)^{1/\alpha_i} \tag{2}$$

where, V represents resistive voltage drop, I represents arrester current, K is constant and α is nonlinearity constant. This V-I characteristic is represented in Fig. 5.

The Surge Arrester block is modeled as a current source driven by the voltage appearing across its terminals. Therefore, it cannot be connected in series with an inductor or another current source. For continuous simulation, in order to avoid an algebraic loop, the voltage applied to the nonlinear resistance is filtered by a first-order filter with a time constant of 0.01 microseconds. This fast time constant does not significantly affect the result accuracy [11].

4 Transformer Core Losses Modeling

In this paper, the core losses model is described by a third order power series which coefficients are fitted to match the hysteresis and eddy current nonlinear characteristics were each term of it is based on voltage and is given in (3). Also, these model coefficients are given in Table 1. Linear core losses are modeled as a linear resistance [24].

$$i_{Rm} = h_0 + h_1 V_m + h_2 V_m^2 + h_3 V_m^3 \tag{3}$$
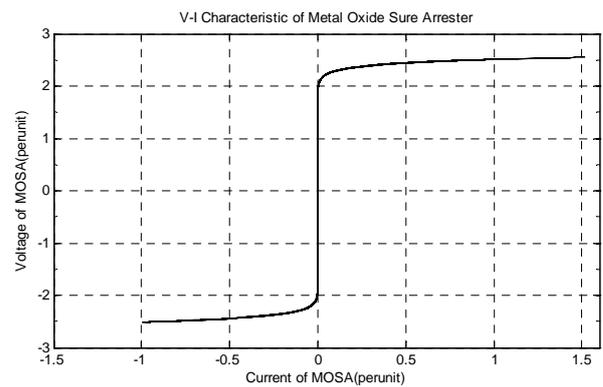
Fig. 5 V-I characteristic of MOSA.

Table 1 Coefficients of nonlinear core model.

h_0	h_1	h_3	h_2
-3.5213E-03	5.7869E-07	-1.4167E-12	1.21105E-18

5 Differential Equations Analysis

The differential equations for the circuit in Fig. 3 are presented as follow:

$$v_1 = \frac{d\varphi}{dt} \tag{4}$$

$$i_c = C\frac{dv_c}{dt}, \quad v_c = E - v_1 \tag{5}$$

$$i_c = i_1 + i_{Rm} \tag{6}$$

$$C\frac{dE}{dt} - C\frac{dv_1}{dt} = \\ h_0 + h_1v_1 + h_2v_1^2 + h_3v_1^3 + (a\varphi + b\varphi^q) + i_{MOSA} \tag{7}$$

$$\frac{dv_1}{dt} = \frac{dE}{dt} - \\ \frac{1}{C}(h_0 + h_1v_1 + h_2v_1^2 + h_3v_1^3) - \frac{1}{C}(a\varphi + b\varphi^q) + \left(\frac{v_1}{k}\right)\alpha \tag{8}$$

where, E is the peak value of the voltage source as shown in Fig. 3, φ is the flux linkage of the transformer, k and α is MOSA coefficient. Typical values of the nonlinear magnetization curve nonlinearity index are given in Table 2. Also, power system parameters value is shown in Table 3.

The initial conditions as calculated from steady-state solution of MATLAB are: $\varphi=0$, $V_1=1.44pu$ where, φ is defined as $x_1(t)$ and $d\varphi/dt$ is defined as a second state variable, $x_2(t)$. Because of the nonlinear equation degree, there are two state variables the same as the nonlinear equation degree, but one nonlinear term is remaining in the power system equation. This term is φ^q and q is nonlinear magnetization curve index. In this paper, nonlinear index value is considered 7, 11. For proper state space usage, nonlinear term is lineared around the initial conditions of the power system. So, for linearization, $x_1(t)$ is lineared around $\varphi=0$, first initial condition and $x_2(t)$ is lineared around $d\varphi/dt=1.44$, second initial condition. According to the

Table 2 Typical value of *q* and its coefficient.

q	Coefficient (a)	Coefficient (b)
7	0.0028	0.0072
11	3.14	0.41

Table 3 Power system parameters considered for simulation.

Parameters	Actual Value	Per Unit Value
V_{base}	635.1kv	-
I_{base}	78.2 A	-
R_{base}	8014 kΩ	-
C	4.9 · F	0.07955 pu
R_{core}	4.5 MΩ	556.68 pu
R_{FLR}	50 k Ω	0.0061 pu

explanation above, the state-space formulation φ and $d\varphi/dt$ as state variables is as given below:

$$\begin{cases} x_1(t) = \varphi \\ v = d\varphi/dt \\ \dot{x}_1(t) = x_2(t) \\ x_2(t) = v \end{cases} \tag{9}$$

By defining state space variables, we have (10).

$$\dot{x}_2(t) = \\ -\frac{1}{C}\left(h_0 + h_1x_2(t) + h_2x_2(t)^2 + h_3x_2(t)^3 + ax_1(t) + bx_1(t)^q\right) + \frac{dE}{dt} \tag{10}$$

and standard form of the state space formulation is given in (11).

$$\begin{bmatrix} \dot{x}_1(t) \\ \dot{x}_2(t) \end{bmatrix} = \\ \begin{bmatrix} 0 & 1 \\ \frac{-a - qb}{C}x_1(t)^{q-1} & \frac{-(h_1 + h_2x_2(t) + h_3x_2(t)^2)}{C} \end{bmatrix}\begin{bmatrix} x_1(t) \\ x_2(t) \end{bmatrix} + \begin{bmatrix} 1 \\ 1 \end{bmatrix}u \tag{11}$$

Input variables base on nonlinear equation is:

$$\begin{bmatrix} u_1 \\ u_2 \end{bmatrix} = \begin{bmatrix} \frac{-h_0}{C} \\ \frac{dE}{dt} \end{bmatrix} \tag{12}$$

Output standard form of the state space is given in (13).

$$y(t) = CX(t) \tag{13}$$

$$y(t) = v(t) = \begin{bmatrix} 0 & 1 \end{bmatrix}\begin{bmatrix} x_1(t) \\ x_2(t) \end{bmatrix} \tag{14}$$

For finding stable points of the power system, matrix A should be solved, so equation (16) shows process of deriving stable and unstable points of the power system from matrix A.

$$\det[\lambda I - A] = 0 \tag{15}$$

$$\det\begin{bmatrix} \lambda & -1 \\ \frac{a + bx_1(t)^{q-1}}{C} & \lambda + \frac{(h_1 + h_2x_2(t) + h_3x_2(t)^2)}{C} \end{bmatrix} = 0 \tag{16}$$

Variables p and q are used only for simplifying. Finally, $\lambda 1, 2$ are two poles of the system and are presented in (18).

$$\begin{cases} p = \frac{(h_1 + h_2(1.41) + h_3(1.41)^2)}{C} \\ q = \frac{a}{C} \end{cases} \tag{17}$$

$$\lambda^2 + p\lambda + q = 0 \qquad \lambda_{1,2} = \frac{-p \pm \sqrt{p^2 - 4q}}{2} \tag{18}$$

Figure 6 shows magnitude and phase of the stable points of power system according to parameters value given in Table 3.
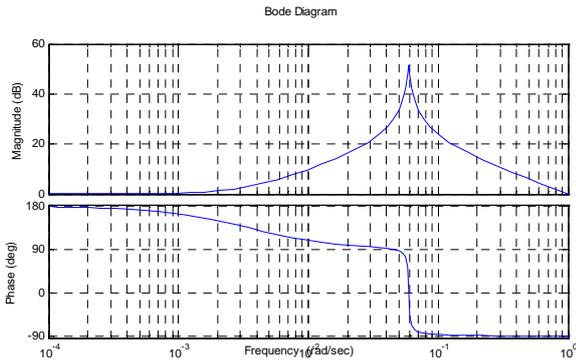
Bode Diagram

Fig. 6 Bode diagram of the given parameters.

6 Power System Modeling Connecting Ferroresonance Limiter

The primary purpose of inserting ferroresonance limiter impedance between the star point of a transformer and earth is to limit earth fault current. The value of impedance required is easily calculated to a reasonable approximation by dividing the rated phase voltage by the rated phase current of the transformer. Ferroresonance limiter impedance is conventionally achieved using resistors rather than inductors, so as to limit the tendency for the fault arc to persist due to inductive energy storage. These resistors will dissipate considerable heat when earth fault current flows and are usually only short term rated, so as to achieve an economic design. Due to the explanation above, In Fig. 7, R_{FLR} is the ferroresonance limiter resistance. Typical values for various system parameters is considered for simulation were kept the same by the case 1, while ferroresonance limiter impedance is added to the power system configuration and its value is given below:

$$R_{FLR} = 50K\Omega$$

Typical values for various system parameters is considered for simulation were kept the same by the case 1, while ferroresonance limiter parameter is added to the system and is given in the Table 3.

The differential equation for the circuit in Fig. 7 is presented in (19).

$$\frac{dv_1}{dt} = \frac{dE}{dt} - \frac{1}{C}\left(h_0 + h_1 v_1 + h_2 v_1^2 + h_3 v_1^3 + a\lambda + b\varphi^q + \left(\frac{v_1}{k}\right)^\alpha\right)$$

$$-R_n.(h_1\frac{dv_1}{dt} + 2h_2 v_1\frac{dv_1}{dt} + 3h_3 v_1^2\frac{dv_1}{dt} + a\frac{d\varphi}{dt} + qb\varphi^{q-1}\frac{d\varphi}{dt}$$

$$+\alpha\left(\frac{1}{k}\right)^\alpha\left(\frac{dv_1}{dt}\right)^{\alpha-1})$$

(19)

where φ is the flux linkage and V is the voltage of transformer.

7 Simulation Results

7.1 Power System Behavior Considering MOSA Effect

The general requirements for ferroresonance are an applied source voltage, a saturable magnetizing inductance of a transformer, a capacitance, and little damping. The capacitance can be in the form of capacitance of underground cables or long transmission lines, capacitor banks, coupling capacitances between double circuit lines or in a temporarily-ungrounded system, and voltage grading capacitors in *HV* circuit breakers [25]. In this section, power system is simulated by considering MOSA. Figs. 8 and 9 show the phase plan diagram of system states with MOSA while value of the power system input voltage is E=3 p.u. Figs. 10 and 11 show the corresponding bifurcation diagrams of the system states with MOSA and including nonlinear core losses effect for *q* = 7, 11 which depicts chaotic behavior.

Power spectrum is shown existence frequencies in the power system behavior. Please see Fig. 7(b).

In Figure 8 input voltage of the power system is plotted against the flux of the power transformer. When the magnitude of the input voltage is 3 p.u, trajectory of the system has subharmonic behavior and amplitude of the flux and overvoltage reaches to 3 p.u. By increasing in the degree of core nonlinearity, *q*, the behavior of the system has being more chaotic as shown in Fig. 8 considering *q* = 11. It is shown chaotic resonance is highly dependent on the transformer nonlinear magnetization cure index.

Figure 9(b) shows subharmonic frequencies in the system. Main harmonic is obvious before 0.5, and other oscillation is after that with lower amplitude. Another tool that can show manner of the system in vast variation of parameters is bifurcation diagram. In Fig. 10, voltage of the system is increased to 6p.u and ferroresonance is begun in 3p.u. Because of the nonlinearity in core losses, ferroresonance began in the big value of the input voltage.
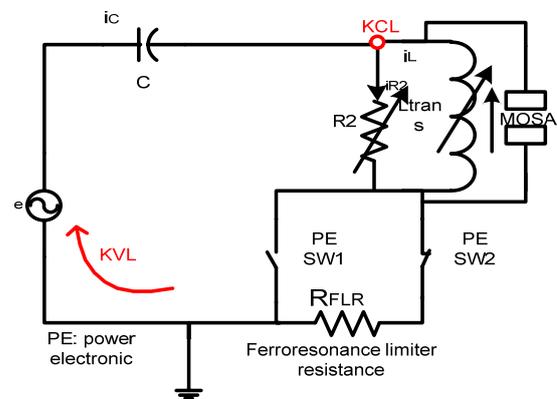

Fig. 7 Equivalent circuit of power system connecting ferroresonance limiter.

Phase plan diagram considering nonlinear magnetization cure index '7', including MOSA effect

(a)

Single-Sided Amplitude Spectrum of voltage on transformer without ferroresonance limiter effect


(b)
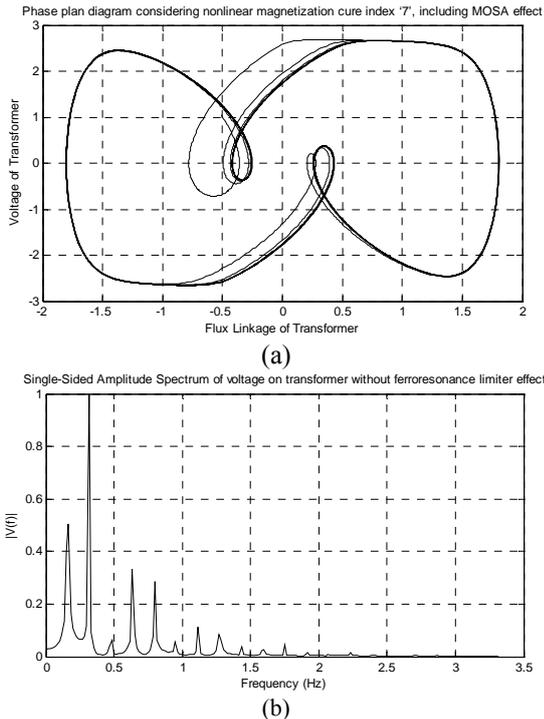
Fig. 8 (a) Phase plan diagram considering nonlinear magnetization curve index '7', including MOSA effect(b) Single-sided amplitude spectrum without considering ferroresonance limiter effect. (Note: In the power spectrum plots, horizontal axis is based on the normalized frequency. It means each 60 Hz is one unit, so when spectrum shows the 3 units, its actual value are 300Hz.)
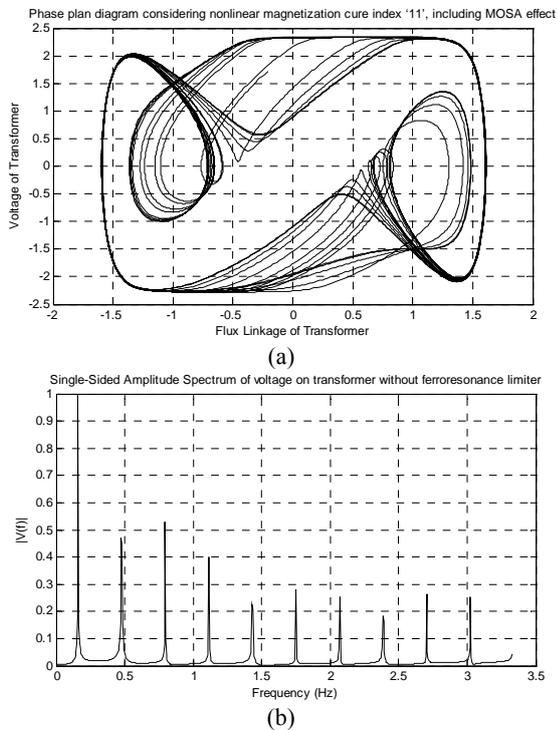
Phase plan diagram considering nonlinear magnetization cure index '11', including MOSA effect

(a)

Single-Sided Amplitude Spectrum of voltage on transformer without ferroresonance limiter

(b)

Fig. 9 (a) Phase plan diagram considering nonlinear magnetization curve index '11', including MOSA effect (b) Single-sided amplitude spectrum without considering ferroresonance limiter effect.

Bifurcation diagram considering nonlinear magnetization cure index '7', including MOSA effect

Fig. 10 Bifurcation diagram considering nonlinear magnetization curve index '7', including MOSA effect.
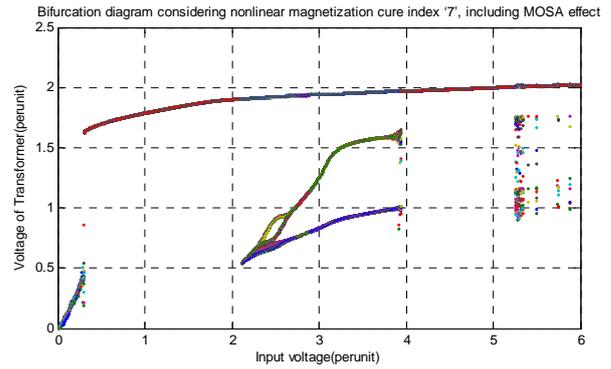
Bifurcation diagram considering nonlinear magnetization cure index '11', including MOSA effect
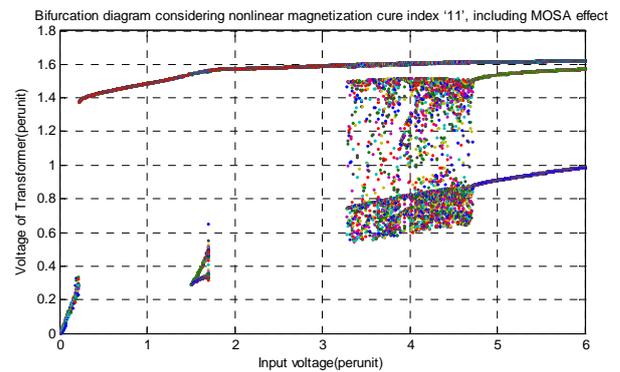
Fig. 11 Bifurcation diagram considering nonlinear magnetization curve index '11', including MOSA effect.

Figure 10 shows the abnormal phenomena in the power transformer considering nonlinear magnetization cure index, q=7. It is clearly shows when q degree changes from 7 to 11, ferroresonance begins in 2 p.u. By comparing Fig. 11 with Fig. 10, it is obvious that margin of beginning ferroresonance is decreased. In Fig. 11, q=11 and amplitude of ferroresonance overvoltage is reached to 1.6 p.u.

7.2 Power System Behavior Considering Ferroresonance Limiter Effect

As shown in the previous part, the nonlinear behavior of ferroresonance falls into two main categories. At first, the response is a distorted periodic waveform, containing the fundamental and higher-order odd harmonics of the fundamental frequency. The second type is characterized by a non-periodic or chaotic response. In both cases the response's power spectrum and simulation results contain fundamental and odd harmonic frequency components. In the chaotic response, however, there are also distributed frequency harmonics and subharmonic resonances. But in this section, effect of ferroresonance limiter on controlling ferroresonance overvoltage is studied and shows this limiter can control ferroresonance overvoltage successfully.

Figures 12 and 13 shows the corresponding phase diagram for the power system modeling is shown in

Figure 7. Also Figures 14 and 15 show the bifurcation diagrams for corresponding system including MOSA and ferroresonance limiter effects. It is shown chaotic regions are controlled by connecting ferroresonance limiter. Also, power spectrum is shown only main harmonic of the power system source frequency.

Single side spectrum in Fig. 13(b) shows fundamental resonances in the case of connecting ferroresonance limiter.

In Figures 14 and 15, system behavior is shown by the proper bifurcation diagram. In Figure 14, the degree of transformer magnetization curve nonlinearity index is 7. This cause to occur one jump in the trajectory of the system and voltage of the transformer is oscillated with period 3 oscillation. In Figure 14, degrees of transformer magnetization curve nonlinearity index to 11. Considering MOSA and ferroresonance limiter cause to remove ferroresonance completely. There are no nonlinear phenomena in the power system and voltage of the transformer has a period 3 oscillation. By increasing the core nonlinearity, behavior remains in periodic oscillation, MOSA and ferroresonance limiter can cause ferroresonance drop out successfully.
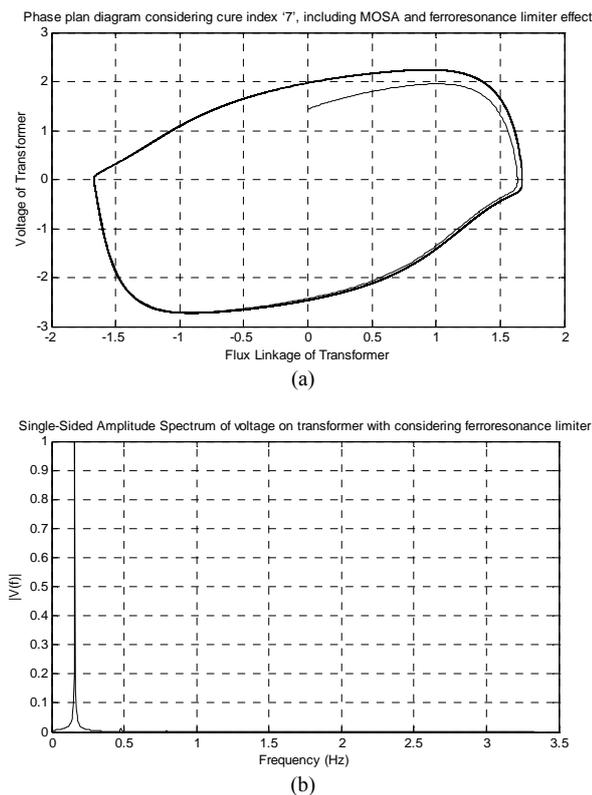
Phase plan diagram considering cure index '7', including MOSA and ferroresonance limiter effect

(a)

Single-Sided Amplitude Spectrum of voltage on transformer with considering ferroresonance limiter

(b)

Fig. 12 (a) Phase plan diagram considering nonlinear magnetization cure index '7', including MOSA and ferroresonance limiter effect (b) Single-sided amplitude spectrum considering ferroresonance limiter effect.


Phase plan diagram considering cure index '11', including MOSA and ferroresonance limiter effect

(a)

Single-Sided Amplitude Spectrum of voltage on transformer with considering ferroresonance limiter

(b)

Fig. 13 (a) Phase plan diagram considering nonlinear magnetization curve index '11', including MOSA and ferroresonance limiter effect (b) Single-sided amplitude spectrum considering ferroresonance limiter effect.
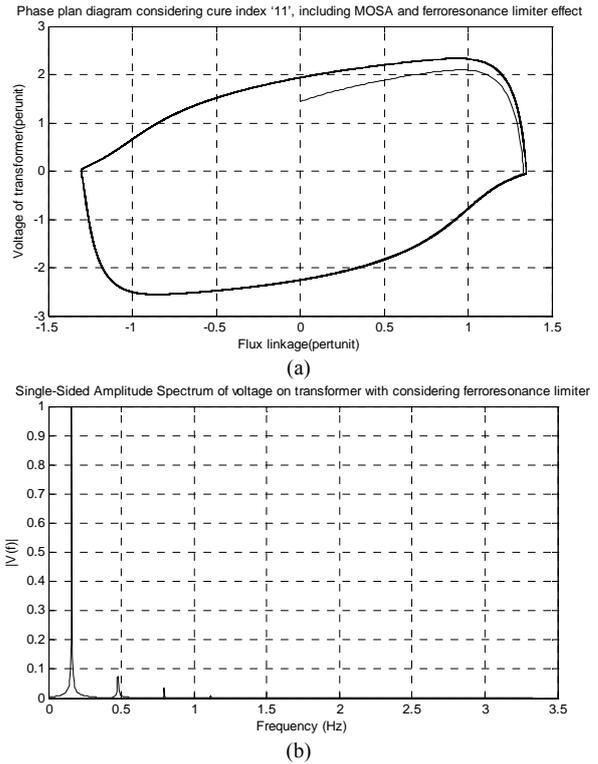
Bifurcation diagram considering curve index '7', including MOSA and ferroresonance limiter effect
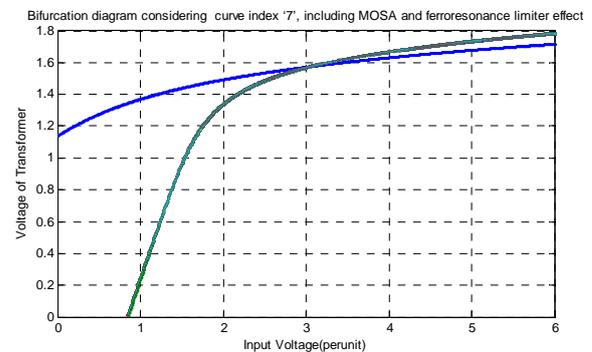
Fig. 14 Bifurcation diagram considering nonlinear magnetization curve index '7', including MOSA and ferroresonance limiter effect.

The use of geometric graphical methods like phase plane projections and bifurcation can be applied to obtain a better understanding of ferroresonance. Ferroresonance in the above three phase nonlinear core distribution transformer can be periodic or non-periodic. Some of the periodic modes of ferroresonance may contain sub-harmonics, but still have strong power frequency components, but take longer than one fundamental cycle to repeat. This occurs more typically for very large values of q. The "higher energy modes" of ferroresonance involving relatively large capacitances and little damping can produce a non-periodic voltage on the open phase(s).

Bifurcation diagram considering curve index '11', including MOSA and ferroresonance limiter effect
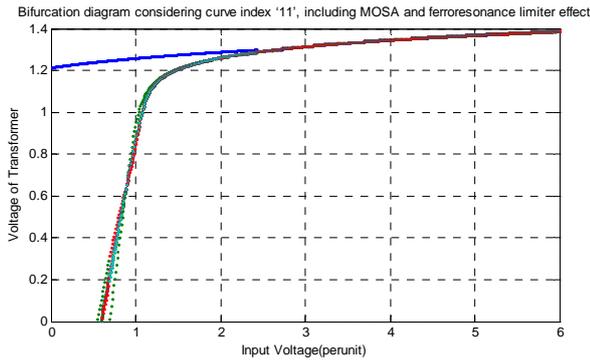
Fig. 15 Bifurcation diagram considering nonlinear magnetization curve index '11', including MOSA and ferroresonance limiter effect.

8 Comparative Discussions

In this paper power transformer is studied with nonlinear core losses model. Then, effect of MOSA and ferroresonance limiter on controlling of nonlinear phenomena and chaos is investigated in deeper cases. In the real system, transformer core has many kind of losses and are strictly nonlinear, the model has been used in this work was chosen from [24]. It has been shown the nonlinear core losses can cause system works better and margin of occurring ferroresonance is decreased as compared with results in [24]. By connecting ferroresonance limiter, ferroresonance overvoltage is ignored and even if unwanted phenomena are appeared, power transformer can works in the safe operation region and there is no dangerous condition in the power system.

9 Conclusions

This paper investigated the ferroresonance oscillation in the power transformer. Ferroresonance in power system makes overvoltage on power equipments and are dangerous phenomena. MOSA is a nonlinear resistance and can cause ferroresonance dropout for some range of system parameters, but MOSA only can limit these overvoltages and cannot control it completely. Ferroresonance limiter is new suggested controlling equipment is connected to the neutral point of the power transformer. It is shown system greatly affected by this limiter. The presence of the ferroresonance limiter results in clamping the ferroresonance non-conventional overvoltages in the power system. This limiter can remove the ferroresonance oscillation completely and system shows less sensitivity to the initial conditions and can work in normal operation conditions.

References

[1] Mork B. A. and Stuehm D. L., "Application of nonlinear dynamics and chaos to ferroresonance in distribution systems", *IEEE Transactions on Power Delivery,* Vol. 9, No. 2, pp. 1009-1017, 1994.

[2] Bethenod J., "Sur le transformateur et résonance" , *L'Eclairae Electrique*, pp. 289-296, Nov. 1907.

[3] Butler J. W. and Concordia C., "Analysis of series capacitor application problems", *AIEE Trans.*, Vol. 56, No. 8, pp. 975-988, 1937.

[4] Emin Z., Al Zahawi B. A. T. and Tong Y. K., "Voltage transformer ferroresonance in 275 kV substation", *Eleventh International Symposium on High Voltage Engineering*, Vol. 1, No. 2, pp. 283-286, 1999.

[5] Andrei R. G. and Halley B. R., "Voltage transformer ferroresonance from an energy transfer standpoint", *IEEE Transactions on Power Delivery*, Vol. 4, No. 3, pp.1773-1778, Jul. 1989.

[6] Li Y., Shi W., Qin R. and Yang J., "A systematical method for suppressing ferroresonance at neutral-grounded substations", *IEEE Transactions on Power Delivery*, Vol. 18, No. 3, pp. 1009-1014, July 2003.

[7] Charalambous C., Wang Z. D., Osborne M. and Jarman P., "Sensitivity studies on power transformer ferroresonance of a 400 kV double circuit", *IET journal of Generation, Transmission & Distribution*, Vol. 2, No. 2, pp. 159-166, March 2008.

[8] Li Y., Shi W. and Li F., "Novel analytical solution to fundamental ferroresonance-part I: power frequency excitation characteristic", *IEEE Transactions on Power Delivery,* Vol. 21, No. 2, pp. 788-793, April 2006.

[9] Jacobson D. A. N., Lehn P. W. and Menzies R. W., "Stability domain calculations of period-1 ferroresonance in a nonlinear resonant circuit", *IEEE Transactions on Power Delivery*, Vol. 17, No. 3, pp. 865-871, Jul. 2002.

[10] Mokryani G. and Haghifam M. R., "Application of wavelet transform and MLP neural network for Ferroresonance identification", *IEEE Conference of Conversion and Delivery of Electrical Energy in the 21st Century*, pp. 1-6, July 2008.

[11] Rezaei-Zare A., Iravani R. and Sanaye-Pasand M., "Impacts of transformer core hysteresis formation on stability domain of ferroresonance modes", *IEEE Transactions on Power Delivery*, Vol. 24, No. 1, pp. 177-186, Jan. 2009.

[12] Charalambous C. A., Wang Z. D., Jarman P. and Osborne M., "2-D Finite-Element Electromagnetic Analysis of an Autotransformer Experiencing Ferroresonance", *IEEE Transactions on Power Delivery*, Vol. 24, No. 3, pp. 1275-1283, July 2009.

[13] Khorasani P. G. and Deihimi A.,"A new modeling of Matlab transformer for accurate simulation of ferroresonance", *International Conference on Power Engineering, Energy and Electrical Drives*, Vol. 1, No. 3, pp. 529-534, March 2009.

[14] Radmanesh H. and Rostami M., "Effect of circuit breaker shunt resistance on chaotic ferroresonance in voltage transformer", *Advances in Electrical and Computer Engineering*, Vol. 10, No. 3, pp. 71-77, 2010.

[15] Radmanesh H., "Controlling Ferroresonance in Voltage Transformer by Considering Circuit Breaker Shunt Resistance Including Transformer Nonlinear Core Losses Effect", *International Review on Modeling and Simulations*, Vol. 3, No. 5, Part A, pp. 988-996, 2010.

[16] Radmanesh H., "Controlling Chaotic Ferroresonance Oscillations in Autotransformers Including Linear and Nonlinear Core Losses Effect", *International Review of Electrical Engineering*, Vol. 5, No. 6, pp. 2644-2652, 2010.

[17] Beiza J., Hosseinian S. H. and Vahidi B., "Fault Type Estimation in Power Systems", *Iranian Journal of Electrical & Electronic Engineering (IJEEE),* Vol. 5, No. 3, pp. 185-195, 2009.

[18] Esmaili M., Shayanfar H. A. and Amjady N.," Stochastic Congestion Management Considering Power System Uncertainties", *Iranian Journal of Electrical & Electronic Engineering (IJEEE)*, Vol. 6, No. 1, pp. 36-47, 2010.

[19] Faghihi F. and Heydari H., "Mathematical proof for the Minimized Stray Fields in Transformers Using Auxiliary Windings Based on State Equations for Evaluation of FEM Results", *Iranian Journal of Electrical & Electronic Engineering (IJEEE),* Vol. 6, No. 1, pp. 62-69, 2010.

[20] Sefidgaran M., Mirzaie M. and Ebrahimzadeh A., "Reliability Model of Power transformer with ONAN Cooling", *Iranian Journal of Electrical & Electronic Engineering (IJEEE)*, Vol. 6, No. 2, pp. 103-109, 2010.

[21] Nemati A. and Pakdel M., "A New ZVZCS Isolated Dual Series Resonant DC-DC Converter with EMC Considerations", *Iranian Journal of Electrical & Electronic Engineering (IJEEE)*, Vol. 6, No. 3, pp. 190-198, 2010.

[22] Abbasi H., Gholami A. and Abbasi A., "Investigation and Control of Unstable Chaotic Behavior Using of Chaos Theory in Two Electrical Power Systems: 1-Buck Converter2-Power transformer", *Iranian Journal of Electrical*

[23] Mozaffari S., Sameti M. and Soudack A. C., "Effect of initial conditions on chaotic ferroresonance in power transformers", *IEE Proceedings/Generation, Transmission and Distribution*, Vol. 144, pp. 456-460, 1997.

[24] Al-Anbarri K., Ramanujam R., Saravanaselvan R. and Kuppusamy K., "Effect of iron core loss nonlinearity on chaotic ferroresonance in power transformers", *Electric Power Systems Research*, Vol. 65, No. 1, pp. 1-12, 2003.

[25] Blackburn J. L., *Protective Relaying Principles and Applications,* New York, NY: Marcel Dekker, Inc., pp. 231-237, 1987.

Hamid Radmanesh was born in 1981. He studied Telecommunication engineering at Malek-Ashtar University of Technology, Tehran, Iran, and received the BSC degree in 2006 also studied electrical engineering at Shahed University Tehran, Iran, and received the MSC degree in 2009. Currently, he is a PhD student in Amirkabir University of Technology. His research interests include design and modeling of power electronic converters, drives, and transient and chaos in power system apparatus.
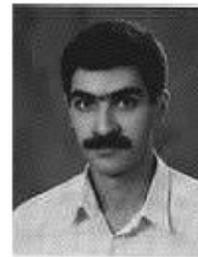
Mehrdad Rostami was born in 1965, Tehran, IRAN. He received BSc, MSc and Ph.D in Electrical engineering from Tehran Polytechnic University (Amir Kabir), Tehran Iran in 1988, 1991 and 2003 respectively. He is currently working as an Assistant professor and vice chancellor in research and development of Shahed University Engineering Faculty, Tehran, IRAN.